Spin State

Deutsche Ausgabe: DOI: 10.1002/ange.201600165
Internationale Ausgabe: DOI: 10.1002/anie.201600165

A Unified Treatment of the Relationship Between Ligand Substituents and Spin State in a Family of Iron(II) Complexes

Laurence J. Kershaw Cook, Rafal Kulmaczewski, Rufeida Mohammed, Stephen Dudley, Simon A. Barrett, Marc A. Little, Robert J. Deeth, and Malcolm A. Halcrow**

Abstract: *The influence of ligands on the spin state of a metal ion is of central importance for bioinorganic chemistry, and the production of base-metal catalysts for synthesis applications. Complexes derived from $[Fe(bpp)_2]^{2+}$ (bpp = 2,6-di{pyrazol-1-yl}pyridine) can be high-spin, low-spin, or spin-crossover (SCO) active depending on the ligand substituents. Plots of the SCO midpoint temperature ($T_{1/2}$) in solution vs. the relevant Hammett parameter show that the low-spin state of the complex is stabilized by electron-withdrawing pyridyl ("X") substituents, but also by electron-donating pyrazolyl ("Y") substituents. Moreover, when a subset of complexes with halogeno X or Y substituents is considered, the two sets of compounds instead show identical trends of a small reduction in $T_{1/2}$ for increasing substituent electronegativity. DFT calculations reproduce these disparate trends, which arise from competing influences of pyridyl and pyrazolyl ligand substituents on Fe-L σ and π bonding.*

The ability of first-row transition ions to adopt different spin states in strong or weak ligand fields is of great importance to their catalysis and reactivity.[1–3] For example, fundamental mechanistic steps in biological and synthetic oxidation catalysis involve a change in spin state at an iron catalyst center, described as two-state reactivity.[3] Catalysts with different resting spin states follow different pathways through these two-state processes, leading to altered reactivity and product distributions.[4] Similar considerations also apply for "base-metal" catalysts for organometallic reactions,[5] which give access to high-spin active species with different reactivity patterns compared to conventional precious-metal catalysts.[6,7] Another consequence of spin-state dichotomy is the phenomenon of spin crossover (SCO), where a molecular or framework compound exhibits a transition between high- and low-spin states under a physical stimulus.[8,9] SCO compounds have been developed into versatile molecular switches for molecular materials chemistry and nanoscience.[9,10]

The relationship between chemical structure and spin state is central to these phenomena.[2,11] A sterically crowded ligand sphere generally leads to high-spin complexes.[12] However, the effect of ligand electronic character on metal-ion spin state is less clear-cut, with electron-withdrawing substituents being reported to stabilize either the low-spin[13–16] or the high-spin state[17,18] in different series of compounds. While the literature includes data from solution and the solid-state, these effects are best quantified by solution measurements which determine a complex's spin state in the absence of crystal-packing effects or any other influences from a rigid solid lattice.[19] We report herein a comprehensive study to resolve this contradiction, through a survey of twenty-five complexes from the $[Fe(bpp^{X,Y})_2]^{2+}$ family ($bpp^{X,Y}$ = a 2,6-di(pyrazol-1-yl)pyridine derivative; Scheme 1).[20] Our results show that substituents at the X and Y sites have different, opposing effects on the iron-atom spin state.

The spin states of these complexes were measured in solution by the variable-temperature Evans method,[21] in $(CD_3)_2CO$ or CD_3NO_2 depending on their solubility (Figure 1). Our use of different weakly interacting solvents should cause only small perturbations to the data.[22] The complexes with $X = NH_2$ and NMe_2 remain high-spin within experimental error over the liquid range of the solvent. All the other complexes exhibit SCO, although the midpoint temperature of the transition ($T_{1/2}$) varies from 158 K (X = OMe) $\leq T_{1/2} \leq$ 305 K (X = NO_2).[23] Where they could be derived, thermodynamic parameters for these equilibria are mostly similar to other $[Fe(bpp^{X,Y})_2]^{2+}$ complexes.[20,23] However, higher ΔH and ΔS values for $[Fe(bpp^{CO_2H,H})_2]^{2+}$ and $[Fe(bpp^{SO_2Me,H})_2]^{2+}$ imply that ligand-dissociation equilibria in those complexes may be occurring, promoted by the nucle-

[*] Dr. L. J. Kershaw Cook, Dr. R. Kulmaczewski, Dr. R. Mohammed, S. Dudley, S. A. Barrett, Dr. M. A. Little, Prof. M. A. Halcrow
School of Chemistry
University of Leeds
Leeds, LS2 9JT (UK)
E-mail: m.a.halcrow@leeds.ac.uk
Prof. R. J. Deeth
Inorganic Computational Chemistry Group
Department of Chemistry
University of Warwick
Coventry, CV4 7AL (UK)
E-mail: r.j.deeth@warwick.ac.uk
Dr. L. J. Kershaw Cook
Current address: Department of Chemistry, University of Bath
Claverton Down, Bath BA2 7AY (UK)
Dr. M. A. Little
Current address: Department of Chemistry, University of Liverpool
Crown Street, Liverpool, L69 7ZD (UK)
Prof. R. J. Deeth
Current address: School of Chemistry, University of Edinburgh,
Joseph Black Building
David Brewster Road, Edinburgh EH9 3FJ (UK)
Supporting information and the ORCID identification number(s) for the author(s) of this article can be found under http://dx.doi.org/10.1002/anie.201600165.

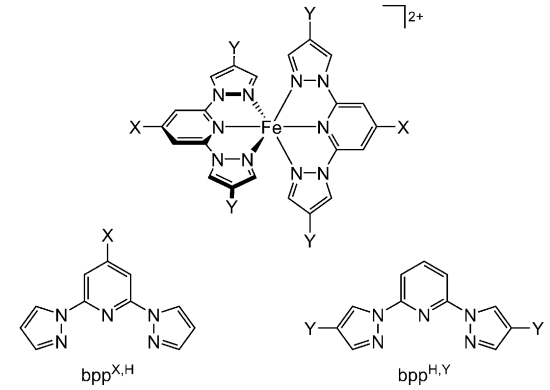

X = H
Me, CH_2SCN, CO_2H,
F, Cl, Br, I
NH_2, NMe_2, NO_2
OH, OMe
SH, SSbpp, SMe, SOMe,
SO_2Me

Y = H
Me, CH_2OH, *t*Bu, CO_2Et
Cl, Br, I

Scheme 1. Different substitution patterns of $[Fe(bpp)_2]^{2+}$ (top), and the different $bpp^{X,Y}$ ligands referred to in this study (bottom).

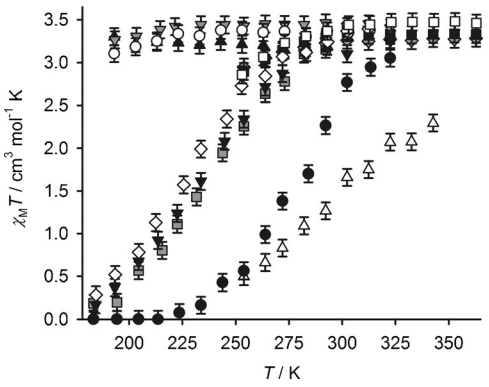

Figure 1. Solution-phase magnetic susceptibilty data: $[Fe(bpp^{OH,H})_2][BF_4]_2$ (○); $[Fe(bpp^{OMe,H})_2][PF_6]_2$ (▼); $[Fe(bpp^{NH_2,H})_2][BF_4]_2$ (▲); $[Fe(bpp^{Me,H})_2][BF_4]_2$ (□); $[Fe(bpp^{F,H})_2][BF_4]_2$ (◆); $[Fe(bpp^{pz,H})_2][BF_4]_2$ (■); $[Fe(bpp^{Cl,H})_2][BF_4]_2$ (◇); $[Fe(bpp^{Br,H_2})][BF_4]_2$ (▼); $[Fe(bpp^{I,H})_2][BF_4]_2$ (■); $[Fe(bpp^{CO_2H,H})_2][BF_4]_2$ (●); $[Fe(bpp^{NO_2,H})_2][BF_4]_2$ (△).[23]

ophilic carboxylic and sulfoxide substituents. Since ligand dissociation only occurs in the labile high-spin state of a complex, as a pre-equilibrium to SCO, it will have little effect on $T_{1/2}$.[19,22]

Plots of $T_{1/2}$ versus the substituent electronegativity (χ^P[24]) for $[Fe(bpp^{X,H})_2]^{2+}$ and $[Fe(bpp^{H,Y})_2]^{2+}$ show identical correlations for substituents with weak π-bonding character (X, Y = halogen and SH; Figure 2). Within this series, electronegative substituents lower $T_{1/2}$ to a small extent, so less electron-rich X and Y groups slightly stabilize the high-spin state. That is consistent with basic ligand-field arguments. However, simple X and Y substituents with π-bonding resonance properties (X, Y = CH_3, NH_2, and OH) deviate strongly from this relationship. That implies metal–ligand π bonding must contribute to the spin states of these complexes.

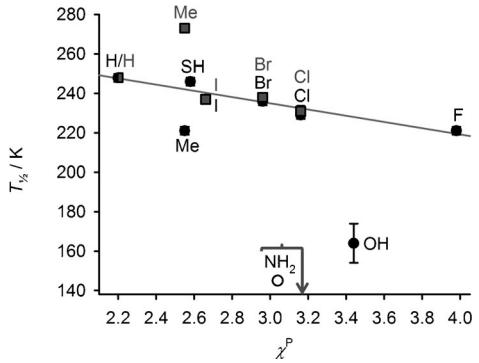

Figure 2. Plot of $T_{1/2}$ versus the substituent electronegativity (χ^P) for $[Fe(bpp^{X,H})_2]^{2+}$ (●) and $[Fe(bpp^{H,Y})_2]^{2+}$ (■) complexes with simple heteroatom X and Y substituents.[23] $T_{1/2}$ for X = NH_2 (○) represents an upper limit for that measurement, since the complex is fully high-spin over the liquid range of the solvent. The line shows the best fit correlation ($R^2 = 0.91$), omitting the X/Y = Me, OH and NH_2 datapoints.

Resonance effects for ligand "X" substituents are accounted for by the σ_p Hammett parameter.[25] A plot of $T_{1/2}$ versus σ_p for $[Fe(bpp^{X,H})_2]^{2+}$ contains some scatter, particularly around $\sigma_p \approx 0$, but shows a positive linear correlation (Figure 3, top). That is, more electron-withdrawing pyridyl X substituents stabilize the low-spin state of $[Fe(bpp^{X,H})_2]^{2+}$. This result is consistent with previous studies of complexes with pyridyl donor ligands,[14–16] but it is the

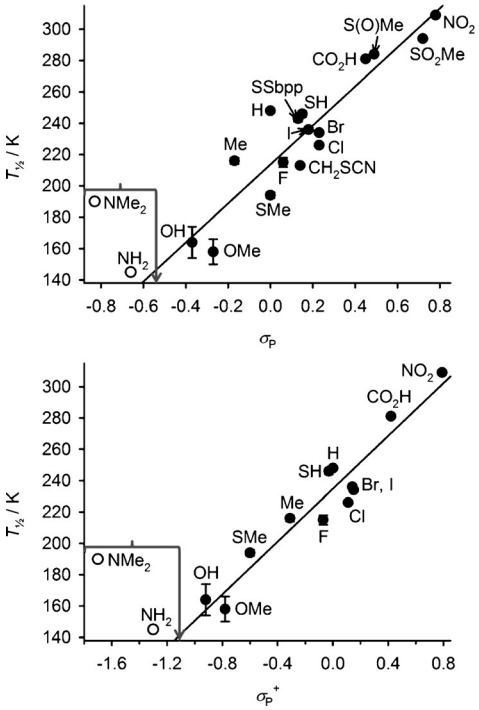

Figure 3. Plots of $T_{1/2}$ for $[Fe(bpp^{X,H})_2]^{2+}$ versus the X substituent Hammett parameters σ_p (top) and σ_p^+ (bottom; Table S1 in the Supporting Information).[23] Error bars are mostly smaller than the symbols on the graph. The lines show the best fit correlation ($R^2 = 0.86$ [top] and 0.92 [bottom]), omitting the X = NH_2 and NMe_2 datapoints (○) which represent the upper limits for those $T_{1/2}$ measurements.

opposite trend to the electronegativity plot (Figure 2). An improved correlation is found when $T_{1/2}$ is plotted against σ_p^+, a modified Hammett parameter accounting for conjugation of the ligand substitutents with a positively charged reaction center (Figure 3, bottom).[25] Hence, these data appear to be influenced by π bonding between the Lewis acidic Fe^{2+} ion and the ligand pyridyl donors. In contrast, a plot of $T_{1/2}$ for $[Fe(bpp^{H,Y})_2]^{2+}$ versus the relevant substituent Hammett parameter (σ_M[25]) shows the opposite trend from the $[Fe(bpp^{X,H})_2]^{2+}$ series. That is, more electron-withdrawing pyrazolyl substituents stabilize the high-spin state in $[Fe(bpp^{H,Y})_2]^{2+}$ derivatives, even when substituent resonance effects are included (Figure 4). Such a dependence of $T_{1/2}$ on the positioning of ligand substituents, in the absence of any steric influence, has not been noted before.

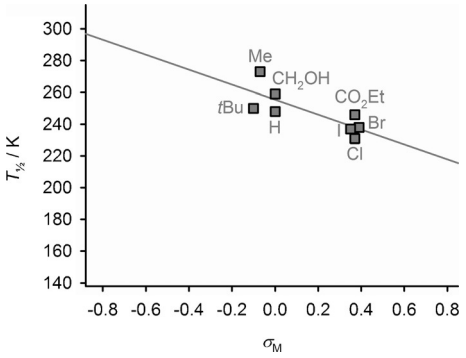

Figure 4. Plot of $T_{1/2}$ versus the Y substituent Hammett parameters σ_M for $[Fe(bpp^{H,Y})_2]^{2+}$ complexes with different Y substituents.[23] Error bars are shown, but are smaller than the symbols on the graph. The line shows the best fit correlation ($R^2 = 0.61$). The graph is drawn for the same range as Figure 3 (top), to aid comparison.

This question was probed by density functional (DFT) calculations of $[Fe(bpp^{X,Y})_2]^{2+}$ using the BP86 functional. The correlation between the measured $T_{1/2}$ and the computed difference between the high-spin and low-spin total energies, ΔE_{rel}(HS-LS), is very good despite the relatively simplistic computational method used,[26] with a R^2 correlation coefficient of 0.79.[23] The agreement between ΔE_{rel}(HS-LS) and the X or Y substituent Hammett parameter is moderate when all the compounds are plotted together, but improves when $[Fe(bpp^{X,H})_2]^{2+}$ and $[Fe(bpp^{H,Y})_2]^{2+}$ are considered separately (Figure 5). Hence, the calculations have captured the spin-state behavior of the two sets of compounds.

The σ and π contributions to Fe–L bonding for each $bpp^{X,Y}$ ligand were quantified by considering the d-orbital energies of the low-spin compounds. Electron-withdrawing X or Y substituents lower the energy of all the metal d-orbitals (Figure 6), but the effect is 2–3 times greater for Y substituents than for X substituents since there as twice as many Y substituents as X groups in a $[Fe(bpp^{X,Y})_2]^{2+}$ molecule. The X substituents in $[Fe(bpp^{X,H})_2]^{2+}$ have a greater effect on the averaged t_{2g} orbital energies than on the e_g orbitals, from the slopes of their least squares correlations (Figure 6). In contrast, Y substituents in $[Fe(bpp^{H,Y})_2]^{2+}$ have a much larger influence on the averaged e_g orbital energies than on the t_{2g} energies (Figure 6).[27]

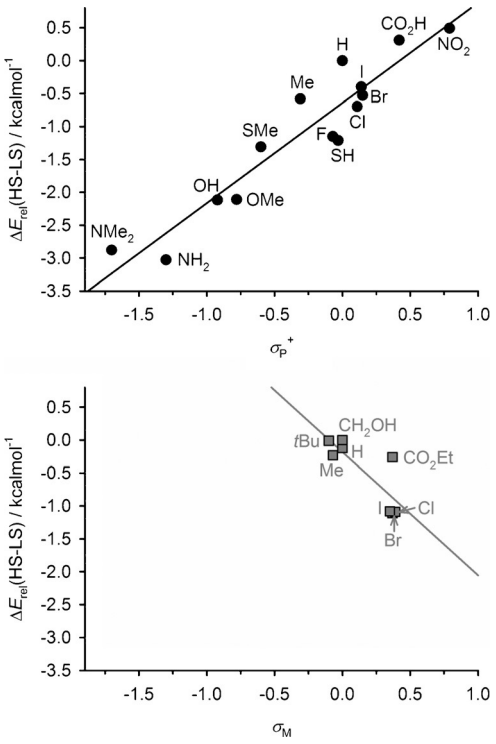

Figure 5. Plot of the relevant substituent Hammett parameter vs. the computed energy difference between the high- and low-spin states relative to X = Y = H [ΔE_{rel}(HS-LS)], for: $[Fe(bpp^{X,H})_2]^{2+}$ (top, ●) and $[Fe(bpp^{H,Y})_2]^{2+}$ (bottom, ■).[23] The graphs are plotted to the same scale to aid comparison, and the lines show the best fit correlations ($R^2 = 0.89$ [top] and 0.67 [bottom][28]).

The relationship between $T_{1/2}$ and the $bpp^{X,Y}$ ligand is a competition between Fe–L σ- and π-bonding effects. Electron-withdrawing substituents inductively lower the energy of the bpp lone pairs, weakening the σ ligand field and thus stabilizing the high-spin state. Conversely, electron-withdrawing substituents also reduce the energy of the $bpp^{X,Y}$ π* MOs, which increases the ligand field by strengthening Fe→bpp π backbonding and favors the low-spin state. Fe–L π-bonding effects dominate in the $[Fe(bpp^{X,H})_2]^{2+}$ series, where electron-withdrawing substituents stabilize the t_{2g} orbital manifold more strongly than the e_g, thus increasing the ligand field and raising $T_{1/2}$. In contrast, the spin state of the $[Fe(bpp^{H,Y})_2]^{2+}$ family is controlled by Fe–L σ bonding, since electron-withdrawing Y substituents stabilize the e_g orbitals more strongly, promoting the high-spin state and lowering $T_{1/2}$.

When complexes with halogen X and Y substituents are considered separately, the stabilization of $E_{av}(e_g)$ by electron-withdrawing substituents is approximately 25% greater than $E_{av}(t_{2g})$ for both sets of complexes.[23] Thus, electronegative halogen X and Y groups both reduce $T_{1/2}$, and the essentially identical $T_{1/2}$ values shown by $[Fe(bpp^{X,H})_2]^{2+}$ and $[Fe(bpp^{H,Y})_2]^{2+}$ when X, Y = a halogen (Figure 2) are also supported by this computational study, despite being contrary to the rest of the data.[17]

These results reconcile the differing conclusions from earlier studies. Electron-withdrawing substitutents indeed

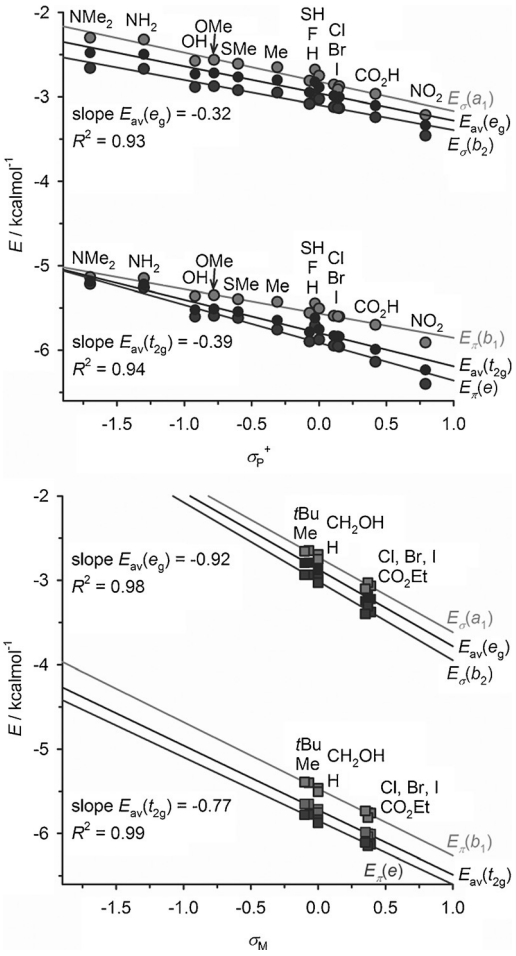

Figure 6. Plot of the relevant substituent Hammett parameter versus the computed d-orbital energies for $[Fe(bpp^{X,H})_2]^{2+}$ (top, circles) and $[Fe(bpp^{H,Y})_2]^{2+}$ (bottom, squares).[23,27] The average orbital energies of the t_{2g} and e_g subshells are also shown, along with their best fit correlations and slopes.

stabilize either the low-spin[13–16] or the high-spin state[17,18] of a complex, depending on their position in the molecule and on which types of substituent are considered. The relationship between ligand design and metal-ion spin state is a fine balance between opposing M–L σ- and π-bonding effects. Rational design of a complex with defined spin-state properties for SCO, catalysis, or other applications requires consideration of all these aspects of the metal–ligand interaction.

Acknowledgements

This work was funded by EPSRC grants EP/H015639/1, EP/F006691/1, EP/K012568/1, EP/K012940/1 and EP/K00512X/1. Support by COST network CM1305 *Explicit Control of Spin States in Technology and Biology* (*ECOSTBio*) and the University of Leeds is also acknowledged. We thank Dr. Oscar Cespedes (University of Leeds) and Dr. Floriana Tuna (University of Manchester) for solid-state magnetic susceptibility data.[23]

Keywords: density functional calculations · iron · N ligands · spin state · substituent effects

How to cite: *Angew. Chem. Int. Ed.* **2016**, *55*, 4327–4331
Angew. Chem. **2016**, *128*, 4399–4403

[1] a) R. Poli, *Chem. Rev.* **1996**, *96*, 2135–2204; b) P. L. Holland, *Acc. Chem. Res.* **2015**, *48*, 1696–1702.
[2] J. N. Harvey, R. Poli, K. M. Smith, *Coord. Chem. Rev.* **2003**, *238–239*, 347–361.
[3] S. Ye, C.-Y. Geng, S. Shaik, F. Neese, *Phys. Chem. Chem. Phys.* **2013**, *15*, 8017–8030.
[4] a) A. R. McDonald, L. Que, Jr., *Coord. Chem. Rev.* **2013**, *257*, 414–428; b) W. Nam, Y.-M. Lee, S. Fukuzumi, *Acc. Chem. Res.* **2014**, *47*, 1146–1154.
[5] a) B. Su, Z.-C. Cao, Z.-J. Shi, *Acc. Chem. Res.* **2015**, *48*, 886–896; b) R. B. Bedford, *Acc. Chem. Res.* **2015**, *48*, 1485–1493; c) R. H. Morris, *Acc. Chem. Res.* **2015**, *48*, 1494–1502.
[6] a) M. P. Shaver, L. E. N. Allan, H. S. Rzepa, V. C. Gibson, *Angew. Chem. Int. Ed.* **2006**, *45*, 1241–1244; *Angew. Chem.* **2006**, *118*, 1263–1266; b) M. P. Johansson, M. Swart, *Dalton Trans.* **2011**, *40*, 8419–8428.
[7] C. Chen, T. R. Dugan, W. W. Brennessel, D. J. Weix, P. L. Holland, *J. Am. Chem. Soc.* **2014**, *136*, 945–955.
[8] a) A. Bousseksou, G. Molnár, L. Salmon, W. Nicolazzi, *Chem. Soc. Rev.* **2011**, *40*, 3313–3335; b) P. Gütlich, A. B. Gaspar, Y. Garcia, *Beilstein J. Org. Chem.* **2013**, *9*, 342–391.
[9] *Spin-crossover materials—properties and applications* (Ed.: M. A. Halcrow), Wiley, Chichester, **2013**, p. 568.
[10] a) M. Cavallini, *Phys. Chem. Chem. Phys.* **2012**, *14*, 11867–11876; b) H. J. Shepherd, G. Molnár, W. Nicolazzi, L. Salmon, A. Bousseksou, *Eur. J. Inorg. Chem.* **2013**, 653–661.
[11] M. A. Halcrow, *Chem. Soc. Rev.* **2011**, *40*, 4119–4142.
[12] See, for example: a) M. G. Simmons, L. J. Wilson, *Inorg. Chem.* **1977**, *16*, 126–130; b) E. C. Constable, G. Baum, E. Bill, R. Dyson, R. van Eldik, D. Fenske, S. Kaderli, D. Morris, A. Neubrand, M. Neuberger, D. R. Smith, K. Wieghardt, M. Zehnder, A. D. Zuberbühler, *Chem. Eur. J.* **1999**, *5*, 498–508; c) J. Elhaïk, D. J. Evans, C. A. Kilner, M. A. Halcrow, *Dalton Trans.* **2005**, 1693–1700; d) V. Martínez, A. B. Gaspar, M. C. Muñoz, G. V. Bukin, G. Levchenko, J. A. Real, *Chem. Eur. J.* **2009**, *15*, 10960–10971.
[13] M. F. Tweedle, L. J. Wilson, *J. Am. Chem. Soc.* **1976**, *98*, 4824–4834.
[14] K. Nakano, N. Suemura, K. Yoneda, S. Kawata, S. Kaizaki, *Dalton Trans.* **2005**, 740–743.
[15] a) I. Prat, A. Company, T. Corona, T. Parella, X. Ribas, M. Costas, *Inorg. Chem.* **2013**, *52*, 9229–9244; b) J. Houghton, R. J. Deeth, *Eur. J. Inorg. Chem.* **2014**, 4573–4580.
[16] K. Takahashi, Y. Hasegawa, R. Sakamoto, M. Nishikawa, S. Kume, E. Nishibori, H. Nishihara, *Inorg. Chem.* **2012**, *51*, 5188–5198.
[17] J. G. Park, I.-R. Jeon, T. D. Harris, *Inorg. Chem.* **2015**, *54*, 359–369.
[18] H.-J. Lin, D. Siretanu, D. A. Dickie, D. Subedi, J. J. Scepaniak, D. Mitcov, R. Clérac, J. M. Smith, *J. Am. Chem. Soc.* **2014**, *136*, 13326–13332.
[19] a) H. Toftlund, *Monatsh. Chem.* **2001**, *132*, 1269–1277; b) B. Weber, F. A. Walker, *Inorg. Chem.* **2007**, *46*, 6794–6803; c) N. Hassan, A. B. Koudriavtsev, W. Linert, *Pure Appl. Chem.* **2008**, *80*, 1281–1292.
[20] M. A. Halcrow, *Coord. Chem. Rev.* **2009**, *253*, 2493–2514.
[21] E. M. Schubert, *J. Chem. Educ.* **1992**, *69*, 62.
[22] S. A. Barrett, C. A. Kilner, M. A. Halcrow, *Dalton Trans.* **2011**, *40*, 12021–12024.
[23] The Supporting Information contains synthetic, crystallographic, and computational procedures, and full characterization data for

the seven new $[Fe(bpp^{X,Y})_2]^{2+}$ complexes; crystallographic Figures and Tables; solution and solid phase magnetic susceptibility data; and Tables and graphs of computed molecular geometries, and spin state and orbital energies.
[24] L. Pauling, *J. Am. Chem. Soc.* **1932**, *54*, 3570 – 3582.
[25] C. Hansch, A. Leo, R. W. Taft, *Chem. Rev.* **1991**, *91*, 165 – 195.
[26] R. J. Deeth, N. Fey, *J. Comput. Chem.* **2004**, *25*, 1840 – 1848.
[27] In the idealized D_{2d} symmetry of the $[Fe(bpp^{X,Y})_2]^{2+}$ molecule, the metal d-orbitals transform as: *e* (d_{xz} and d_{yz}); b_1 ($d_{x^2-y^2}$, which has M–L π symmetry in the axis frame used); b_2 (d_{xy}, a M–L σ symmetry orbital in this axis frame); and, a_1 (d_{z^2}). O_h symmetry labels are used when the σ- and π-symmetry metal d orbitals are discussed collectively.
[28] The weaker agreement between ΔE_{rel}(HS-LS) and σ_M for the $[Fe(bpp^{H,Y})_2]^{2+}$ series reflects an outlier data point for Y = CO_2Et (Figure 5). Anomalous spin-state energies were also calculated for a carboxy-substituted member of a family of iron(II) complexes of pyridyl-containing macrocyclic ligands.[15b]

Received: January 6, 2016
Published online: March 1, 2016

